

On the geometrical structure of the C_3^+ cation—an *ab initio* study

J. M. L. Martin^{a)} and J. P. François

Limburgs Universitair Centrum, Department SBM, Universitaire Campus, B-3610 Diepenbeek, Belgium

R. Gijbels

University of Antwerp (UIA), Institute for Materials Science, Department of Chemistry, Universiteitsplein 1, B-2610 Wilrijk, Belgium

(Received 30 March 1990; accepted 18 June 1990)

The potential energy surface of the C_3^+ cation has been investigated using coupled cluster techniques and large basis sets. The results are particularly sensitive towards the level of electron correlation. Spin contamination even produces a “false stationary point” at the UHF/6-31G* level. C_3^+ has a cyclic 2B_2 ground state with predicted geometry $r = 1.3242 \text{ \AA}$, $\theta = 73.06^\circ$ (MP2/6-311G*, empirically corrected bond distance). At the highest level of theory considered, the linear structure (${}^2\Sigma_u^+$ state) lies about 2 kcal/mol above the ground state: this might imply quasilinearity. There is also a low barrier towards degenerate isomerization: at high temperatures, C_3^+ will be extremely floppy. Harmonic frequencies (UHF/6-31G*) as well as double-harmonic IR and Raman intensities are given for various structures of C_3^+ . Interesting analogies of C_3^+ with B_3 and B_2N are pointed out. The heat of formation at 298.15 K, vertical and adiabatic ionization potentials of C_3 are predicted as $194.9 \pm 2 \text{ kcal/mol}$, $11.92 \pm 0.1 \text{ eV}$, and $11.84 \pm 0.1 \text{ eV}$, respectively.

I. INTRODUCTION

Considerable attention has gone in recent years to the structure and energetics of carbon clusters. The situation up to April 1989, as well as the high significance of this subject, have been reviewed by Weltner and Van Zee.¹ Since then, additional progress has been made, including definitive IR-spectroscopic characterizations of C_4 and C_5 by an interaction between theory²⁻⁵ and experiment.^{6,7}

The situation is less clear for the ions than for the neutral clusters. C_3^+ is believed to be the building block for the larger clusters;⁸ however, its geometrical structure is unknown to date. Previous theoretical studies always assumed a linear structure (see e.g. Ref. 9) by analogy with the neutral species.

Recently, C_3^+ has been investigated¹⁰ using the Coulomb explosion technique.¹¹ The results indicate a cyclic structure; preliminary *ab initio* calculations by Raghavachari (private communication quoted in Ref. 10) appear to confirm this. However, Vager and Kanter¹² remarked that the experimental intensity distributions¹⁰ could also be rationalized under the assumption of a linear structure with an extremely low bending frequency (as C_3 is since long known to have¹³) with a “hot” (about 450 K) Boltzmann distribution. We therefore thought it was worthwhile to perform a high-level *ab initio* study on these species, which might help to settle the issue.

II. COMPUTATIONAL METHODS

The major part of the calculations was performed using the GAUSSIAN 88 program system¹⁴ running on a VaxStation 2000 under VMS 4.7. Some calculations with larger basis sets (MP2 geometry optimizations with the 6-311G* basis

set, coupled cluster calculations with the 6-311 + G* basis set) were too demanding for the VaxStation in terms of both disk space and CPU requirements. These were performed using GAUSSIAN 86¹⁵ running on an IBM 4381/FPS-X64 configuration at the Facultés Universitaires de Namur. Finally, the largest coupled cluster calculations in the 6-311G(2df) basis set (90 contracted Gaussians, all valence electrons correlated in 87 orbitals) were performed using GAUSSIAN 86 on the IBM 3090/400e VF (running under MVS/XA) at the K. U. Leuven.

Firstly, the potential energy surface was investigated at the UHF/6-31G* level using analytical first and second derivatives.¹⁶ Energy separations between the various stationary points were evaluated using the QCISD(T) model,¹⁷ which is actually an approximation to CCSD (coupled cluster theory¹⁸ with all single and double substitutions¹⁹) with a perturbative triples correction. It was shown very recently²⁰ that QCISD is quite comparable to CCSD for nonpathological cases. During the course of the QCISD calculation, MP2,²¹ MP3,²² and MP4(SDQ)²³ energies, as well as their spin-projected counterparts,²⁴ are obtained “on the fly”; these allow for assessment of convergence of the MBPT series as well as of spin contamination effects.

For the most stable states, geometries were then optimized at the MP2 level using the 6-311G* basis set²⁵ and analytical gradients.¹⁶ From these geometries, both QCISD(T) and CCD + ST(CCD)²⁶ calculations were performed. [In keeping with the recent nomenclature for perturbatively corrected coupled cluster methods,²⁷ we will henceforth denote CCD + ST(CCD) as CCD(ST)]. The latter method was available on the FPS configuration as well as on the IBM 3090, and could thus be used with much larger basis sets. The prime difference with QCISD(T) is in the account for infinite-order single substitution effects and coupling terms thereof: comparison allows their assessment.

^{a)} Also at the University of Antwerp.

Using the CCD(ST) model, calculations were then performed with the 6-311 + G* basis set²⁸ to assess the effect of diffuse functions, and with the 6-311G(2df) basis set²⁹ to evaluate the effect of polarization set expansion. On these final energies, a G1 correction³⁰ was applied to obtain dissociation energies accurate to about 2 kcal/mol.³⁰

III. RESULTS AND DISCUSSION

A. Potential energy surface of C_3^+

Equilibrium geometries obtained at the UHF/6-31G* level are depicted in Figure 1. For these same structures, total energies at various levels of electron correlation, as well as the relative energies with respect to the lowest-lying state, are given in Table I. Electronic configurations, term symbols, and expectation values for the \hat{S}^2 operator are presented in Table II, whereas harmonic frequencies at the UHF/6-31G* level, as well as the corresponding double-harmonic infrared and Raman intensities, are listed in Table III.

It can immediately be seen that electron correlation effects are very prominent for this system. Even qualitative conclusions such as the nature of the ground state are profoundly affected by the electron correlation model selected.

At the Hartree-Fock level, the quartet surface appears to be the lowest one. The equilateral triangle is the ground state, followed at 15.34 kcal/mol by the linear structure C3P002. The latter has the low bending frequency now familiar for linear carbon clusters, which also undergoes a "weak" Renner-Teller splitting here. This implies that there will be another low-lying D_{3h} state C3P001' (${}^2A_2'$), which correlates with the other component of the Renner-Teller

pair. The potential energy surface (PES) is thus markedly similar to the doublet surface of B_3 .³¹ However, the very heavy spin contamination that was seen in both the ${}^2\Pi_g$ and the ${}^2A_1'$ states of B_3 ³¹ is absent here, apparently because the additional two unpaired electrons fill up the low-lying virtual orbitals that cause the problem in B_3 (π_g for the ${}^2\Pi_g$ state, e'' for the ${}^2A_1'$ state).

The doublet surface is considerably higher in energy at the UHF level. For the triangular structure (a ${}^2E'$ state), the Jahn-Teller theorem applies. This leads to two isocles triangles, namely the 2B_2 state C3P004 (apex angle 66.63°) and the 2A_1 state C3P005 (apex angle 49.98°). However, whereas C3P004 is a local minimum, C3P005 is a first-order saddle point on the PES. The latter will be the transition state for a degenerate isomerization between the three equivalent Jahn-Teller distortions of the equilateral triangle: this situation is peculiarly akin to that in B_3 (cf. the 4B_1 and 4A_2 states there), and, to a lesser extent, to the degenerate isomerization of the ${}^1\Sigma_g^+$ state in neutral C_3 (which has a ${}^1E'$ Jahn-Teller state).³³ The linear ${}^2\Sigma_u^+$ state (C3P003), which has the same electronic configuration as the ground state of B_2N , lies much higher in energy at the UHF level, and is also a transition state.

It was only at a much later stage that an additional stationary point C3P006 for the 2B_2 state was accidentally discovered. It lies much higher in energy than C3P004 at the UHF level; however, it is definitely much lower in energy at all levels of electron correlation, having a markedly higher correlation energy. Incidentally, C3P004 has an extremely high degree of spin contamination, which is only modest in C3P006. As the stationary point geometry of C3P004 resembles that of the quartet state C3P001, which is much lower in energy than C3P006, we believe that C3P004 is an artifact of the UHF method, caused by admixture of a lower-lying 4A_1 state which is essentially a distortion of C3P001. The Mulliken charge distributions³⁴ in Fig. 2 clarify this point: those of C3P004 are almost those of an equilateral triangle, whereas C3P006 has a significantly lowered positive charge on the apical C atom.

Similar "false stationary points" were encountered by the authors in a PES study of B_4 ,³⁵ and may be encountered for other molecules. A trick for locating the "true" state which may sometimes work is thus to find the equilibrium geometry of the contaminating state, and then restart the geometry optimization for the state to be located with a geometry significantly different from that of the contaminant, but still reasonable for the target state.

The rationale behind preferring C3P006 over C3P004 is somewhat comparable to that behind the annihilated UHF method of Baker;³⁶ an older paper by Farnell *et al.*³⁷ is also worth mentioning here. In the latter reference, an asymmetric solution with high spin contamination was invariably found to yield poor geometry predictions for homonuclear diatomics; this problem was completely remedied by enforcing symmetry on the wavefunction, which incidentally also greatly reduced spin contamination.

At all levels of electron correlation except MP2 (where C3P003 lies lowest in energy), C3P006 is found to be the ground state.

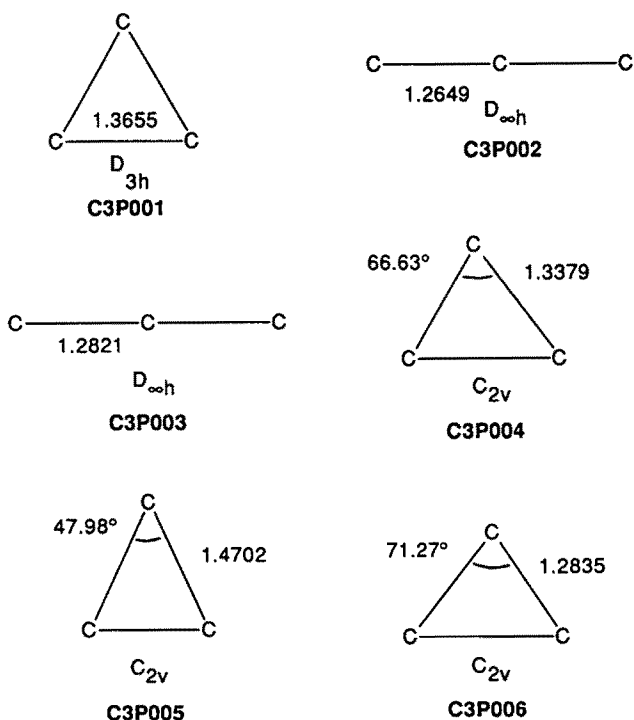


FIG. 1. Stationary point geometries for C_3^+ at the UHF/6-31G* level. Bond distances are in angstrom units.

TABLE I. Total (hartree; minus sign omitted) and relative (kcal/mol) energies using the 6-31G* basis set for various UHF/6-31G* structures of C_3^+ .

Species	UHF	MP2	MP3	MP4(D)	MP4(DQ)	MP4(SDQ)
Total energies						
$C^+(^2P)$	37.28708	37.33107	37.34585	37.35206	37.35124	37.35143
$C(^3P)$	37.68086	37.73297	37.74636	37.75064	37.74979	37.74998
$2C + C^+$	112.64880	112.79702	112.83858	112.85334	112.85083	112.85138
C3P001	112.98376	113.25712	113.27209	113.27946	113.27139	113.27641
C3P002	112.95931	113.20552	113.22180	113.22884	113.22165	113.22980
C3P003	112.89324	113.29561	113.25053	113.29112	113.26608	113.29094
C3P004	112.94226	113.24907	113.26191	113.27285	113.26245	113.27297
C3P005	112.93582	113.24156	113.25482	113.26593	113.25641	113.26582
C3P006	112.93084	113.28199	113.28359	113.29139	113.28388	113.29139
Species	PUHF	PMP2	PMP3	QCISD	QCISD(T)	
$C^+(^2P)$	37.28948	37.33214	37.34625	37.35528	37.35599	
$C(^3P)$	37.68260	37.73383	37.74673	37.75184	37.75277	
$2C + C^+$	112.65467	112.79979	112.83972	112.85896	112.86153	
C3P001	112.98697	113.25882	113.27297	113.28015	113.29745	
C3P002	112.97228	113.21646	113.22989	113.24155	113.25833	
C3P003	112.89959	113.29959	113.25249	113.28266	113.32360	
C3P004	112.96398	113.27033	113.28173	113.29411	113.32128	
C3P005	112.95299	113.25694	113.26699	113.28982	113.31463	
C3P006	112.93811	113.28778	113.28731	113.29680	113.32361	
Relative energies						
Species	UHF	MP2	MP3	MP4(D)	MP4(DQ)	MP4(SDQ)
$2C + C^+$	210.19	312.87	279.25	274.87	271.75	276.11
C3P001	0.00	24.15	7.22	7.48	7.84	9.40
C3P002	15.34	56.53	38.78	39.25	39.05	38.65
C3P003	56.80	0.00	20.75	0.17	11.17	0.28
C3P004	26.04	29.20	13.61	11.63	13.45	11.56
C3P005	30.08	33.92	18.06	15.98	17.24	16.04
C3P006	33.21	8.55	0.00	0.00	0.00	0.00
Species	PUHF	PMP2	PMP3	QCISD	QCISD(T)	
$2C + C^+$	208.52	313.63	280.87	274.74	289.96	
C3P001	0.00	25.58	9.00	10.45	16.41	
C3P002	9.22	52.17	36.03	34.67	40.96	
C3P003	54.83	0.00	21.85	8.87	0.00	
C3P004	14.42	18.36	3.50	1.69	1.46	
C3P005	21.32	26.76	12.75	4.38	5.63	
C3P006	30.66	7.41	0.00	0.00	0.00	

Introduction of electron correlation favors the doublet over the quartet, as expected. Less obvious is that the linear structure C3P003 gets favored by some 30 kcal/mol over C3P004 at the MP2 level. The sequence found here is $C3P002 > C3P005 > C3P001 > C3P006 > C3P003$. Except

for the position of C3P003, this sequence is found at all subsequent levels of theory. At the MP3 level, C3P003 seats itself between C3P002 and C3P005. At the MP4(D) level, C3P003 is situated very close (0.17 kcal/mol) to the ground state. This phenomenon is primarily caused by heavy oscillations

TABLE II. Expectation values of \hat{S}^2 , term symbols, and configurations for various structures of C_3^+ . $\langle S^2 \rangle$, $\langle S^2 \rangle_1$, and $\langle S^2 \rangle_A$ represent the expectation values of \hat{S}^2 for the UHF wave function, the first-order MBPT wave function, and the PUHF wave function, respectively.

Species	$\langle S^2 \rangle$	$\langle S^2 \rangle_1$	$\langle S^2 \rangle_A$	Term	Electronic configuration
C3P001	3.765	3.751	3.750	4A_1	$(a_1')^2(e')^4(a_1')^2(e')^4(a_2')^2(a_1')^2(e')^2$
C3P002	3.991	3.913	3.759	$^4\Pi_u$	$(\sigma_g)^2(\sigma_u)^2(\sigma_g)^2(\sigma_u)^2(\pi_u)^4(\sigma_g)(\sigma_u)(\pi_g)$
C3P003	0.780	0.757	0.750	$^2\Sigma_u^+$	$(\sigma_g)^2(\sigma_u)^2(\sigma_g)^2(\sigma_u)^2(\pi_u)^4(\sigma_g)^2(\sigma_u)$
C3P004	1.495	1.459	0.917	2B_2	$(a_1)^2(b_2)^2(a_1)^2(a_1)^2(a_1)^2(b_2)^2(a_1)^2(b_1)^2(b_2)$
C3P005	1.038	0.977	0.760	2A_1	$(a_1)^2(b_2)^2(a_1)^2(a_1)^2(a_1)^2(b_2)^2(a_1)^2(b_1)^2(a_1)$
C3P006	0.807	0.783	0.752	2B_2	$(a_1)^2(b_2)^2(a_1)^2(a_1)^2(a_1)^2(b_2)^2(a_1)^2(b_1)^2(b_2)$

TABLE III. Harmonic frequencies for various structures of C_3^+ . The numbers between parentheses are the IR intensities (km/mol) and Raman activities ($\text{\AA}^4/\text{a.m.u.}$) within the double-harmonic approximation.

Species	ω_4 (cm^{-1})	ω_3 (cm^{-1})	ω_2 (cm^{-1})	ω_1 (cm^{-1})	ZPE (kcal/mol)
			UHF/6-31G*		
C3P001		1327(e' ,34,1)	1327(e' ,34,1)	1774(a' ,0,50)	6.33
C3P002	233(π_u ,23,0)	330(π_u ,16,0)	1380(σ_g ,0,35)	1956(σ_u ,543,0)	5.57
C3P003	145i(π_u ,18,0)	145i(π_u ,18,0)	1301(σ_g ,0,124)	2496(σ_u ,3932,0)	5.43
C3P004		767(b_2 ,56,19)	891(a_1 ,43,86)	1500(a_1 ,1,20)	4.51
C3P005		89i(b_2 ,132,91)	1080(a_1 ,29,14)	2057(a_1 ,6,470)	4.48
C3P006		793(a_1 ,18,302)	1690(b_2 ,1106,241)	1893(a_1 ,20,505)	6.26
			UHF/6-311G*		
C3P003	163i(π_u ,16,0)	163i(π_u ,16,0)	1286(σ_g ,0,129)	2480(σ_u ,4056,0)	5.38
C3P006		787(a_1 ,17,499)	1668(b_2 ,1203,230)	1868(a_1 ,23,568)	6.18
			UHF/6-31G(2d)		
C3P003	228i(π_u ,8,0)	228i(π_u ,8,0)	1288(σ_g ,0,106)	2463(σ_u ,3769,0)	5.36
C3P006		752(a_1 ,17,390)	1695(b_2 ,1147,118)	1845(a_1 ,20,506)	6.14

tion in the MP series for C3P003 (cf. Table I). At the MP4(DQ) level then, C3P003 and C3P001 change places, whereas the introduction of fourth-order single excitations brings C3P003 close (0.28 kcal/mol) to the ground state again. It is apparent, that coupled-cluster calculations are indispensable here, because the MP series is far from converged at fourth order.

Application of Schlegel's spin projection technique has a rather profound effect. Neglecting the artifact C3P004, the ordering of structures remains unchanged. Both C3P004 and C3P005 apparently benefit greatly; for the same reason as C3P004, the latter also suffers from high spin contamination,

which is however removed for the greatest part by a single spin annihilation (cf. Table II). The barrier height for degenerate isomerization is very strongly reduced by the spin projection.

This conclusion is confirmed when higher-order effects are included by the QCISD(T) procedure. A relatively large barrier between C3P006 and C3P003 is found at the QCISD level: the inclusion of triple excitations flattens it so much that the two structures are energetically degenerate at the QCISD(T) level. The C3P001–C3P006 separation is also significantly increased through the triple excitations (see Table I), which are much more important for C3P003 and C3P004/6 than they are for C3P001 (cf. Table I). (Their effect on the C3P001-ground state of B_3 is not that large either). Both QCISD and QCISD(T) find C3P004 only slightly higher in energy than C3P006, about the amount one would expect from a purely geometric distortion. This attests the capability of CCSD-type methods to correct even very heavy spin contamination, as well as the very high significance of higher-order single excitation effects for spin-contaminated species.^{38,39}

The C3P002–C3P003 pair does exhibit some analogy with the $^2\Sigma_u^+ - ^4\Pi_u$ pair in B_2N .³¹ As can be seen from Fig. 2, C3P003 has the same very polar charge distribution as B_2N in its ground state. It also has an extremely intense asymmetric stretch, just as the ground state of B_2N . The changes in the harmonic frequencies between C3P003 and C3P002 strongly parallel those in B_2N too. The bending frequency of the $^2\Sigma_u^+$ state of B_2N was extremely low: here it is imaginary. The infrared intensity of the asymmetric b_2 stretch of C3P006 is significantly lower than that of the σ_u stretch of C3P003, due to the much more even charge distribution. It is however still about as strong as the intense 2164 cm^{-1} band of C_3 , quite unlike C3P004, which only exhibits a relatively weak b_2 IR intensity.

The σ_u HOMO of C3P003 correlates with the b_2 HOMO of C3P004/C3P006. Its negative orbital energy decreases markedly from C3P003 to C3P006. Note that the Koopmans electron affinity of C3P003, 11.69 eV (σ_u , leading to the $^2\Sigma_g^+$ ground state of C_3) is in unexpectedly good

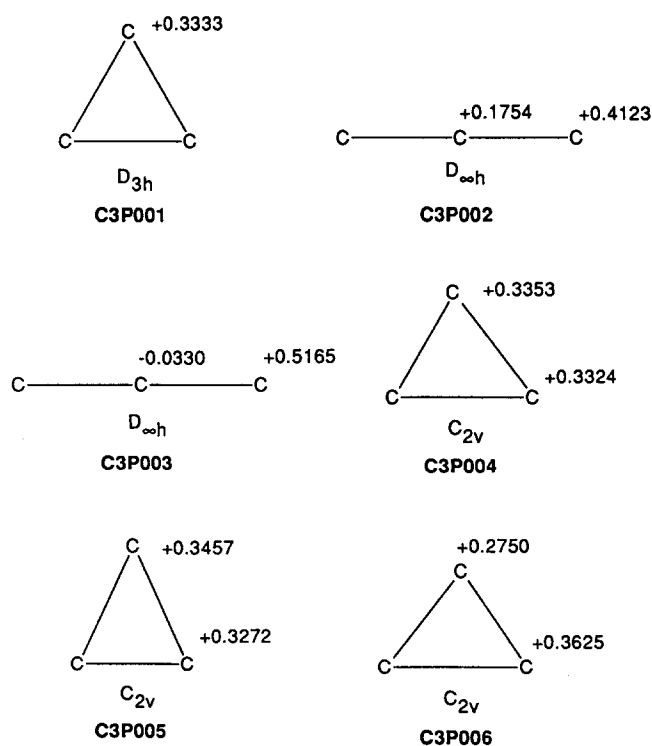


FIG. 2. Mulliken charge distributions (UHF/6-31G*).

agreement with the most reliable vertical IP⁹ for C_3 of 11.46 eV. C3P006 has three low-lying virtual orbitals: 9.33 eV (b_2 , leading to a 1A_1 state that will spontaneously stretch itself to the linear ground state³³), 9.23 eV (a_1 , leading to a 3B_2 state which is a distortion of the $^3A_2'$ equilateral triangle of C_3), and 8.62 eV (a_1 , leading to the corresponding open-shell singlet). C3P001 has a Koopmans EA of 8.32 eV (a_1' , leading to the $^3A_2'$ state).

Subsequently, calculations using both the 6-311G* and 6-31G(2d) basis sets were performed. All conclusions at the 6-31G* level are confirmed. The imaginary frequency of the linear structure is even increased (cf. Table III), so C3P003 will certainly be a transition state at the Hartree-Fock limit. C3P006 is lower in energy than C3P003 at all levels of electron correlation except MP2. However, triple excitations again have a profound effect on the barrier, leading to the conclusion that C_3^+ might perhaps be quasilinear: the energy difference might be so small that a few vibrational quanta suffice to obtain a linear structure. However, for a more serious estimate of the barrier, a correlated reference geometry is necessary.

As expected, the bond distances are significantly lengthened at the MP2/6-311G* level (cf. Fig. 3). An especially spectacular change of 0.0467 Å is seen for C3P006: that for C3P003 is more modest at 0.0264 Å. The bond angle of C3P006 is increased by 1.55°. At these reference geometries, the degree of spin contamination is rather small

($\langle S^2 \rangle = 0.785$ and 0.782 for C3P003 and C3P006, respectively; for the first-order MBPT wave function, we found 0.760 and 0.761), as well as being almost equal for the two species. It might then be that higher-order single excitation effects cancel between the two. This assumption was tested by running both CCD(ST) and QCISD(T) calculations from both geometries. As witnessed from Table IV, the differences indeed cancel to some extent. This enables us to use CCD(ST) (which was available on the FPS system) for the larger basis set calculations.

One might not expect MP2/6-311G* geometries to be accurate because of the significance of higher-order effects. However, MP2/6-31G* performed quite well for geometries and harmonic frequencies of other carbon clusters.²⁻⁵ In general, MP2/6-31G* $A-B$ bond distances tend to be overestimated;⁴⁰ enlargement of the basis set diminishes the effect.⁴¹ In cases with spin contamination, infinite-order single excitations tend to lengthen the bond distances;³⁹ however, for the small contamination mentioned in the previous paragraph the effect would amount to a few thousandths of an angstrom at most. As both effects are of the same order of magnitude and work in opposite directions, some error cancellation will occur. This is just as well, since QCISD or QCISD(T) geometry optimizations were out of the question with the present computer facilities. For our main purpose, which is the evaluation of energies, the geometries will certainly be accurate enough.

The assumption was tested anyway with the 6-31G* basis set for C3P003, by computing the energy at five points 1.26(0.015)1.32. Equilibrium geometries obtained (3 decimal places maximum accuracy) were 1.306 Å at the MP2 level, 1.307 Å at the QCISD level, and 1.318 Å at the QCISD(T) level. Enlargement of the basis set will tend to shorten the computed bond distance, so the MP2/6-311G* geometry might be close to one obtained, say, at the QCISD(T)/6-311G(2df) level.

Faibis *et al.*¹⁰ obtained an R_s distribution in their Coulomb explosion measurements, with R_s being defined as

$$R_s = \frac{v_a + v_b}{v_c}, \quad (1)$$

where v_a , v_b , and v_c represent the velocities of the three fragment ions with respect to the center of mass, ordered as $v_a < v_b < v_c$. For an isosceles triangle, one finds

$$R_s = 1 + \frac{2}{\sqrt{(1 + 9 \tan^2(\theta/2))}}, \quad (2)$$

where θ represents the apex angle of the triangle. A rigid linear structure would correspond to $R_s = 1$; a rigid D_{3h} structure to $R_s = 2$. The MP2/6-311G* equilibrium geometry for C3P006 leads to an R_s value of 1.821, in excellent agreement with the experimental distribution¹⁰ which peaks around $R_s = 1.82$.

Attempts to compute MP2 harmonic frequencies by finite differences of the gradient failed, because of SCF convergence difficulties in the displaced geometries. As anharmonicity and rotation-vibration coupling are prone to be quite large for this molecule, we plan to perform an energy grid calculation, and subsequently an anharmonic analysis,

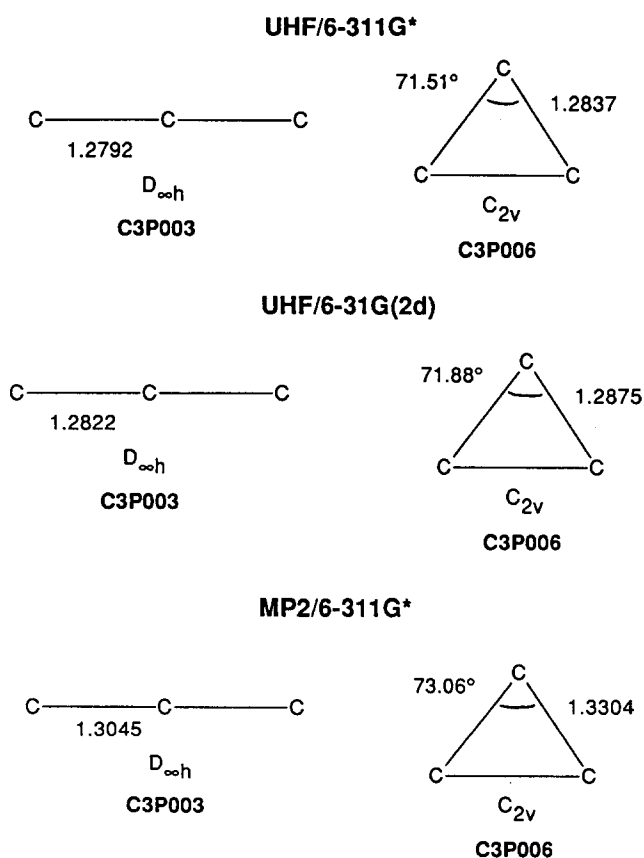


FIG. 3. Stationary point geometries for C3P003 and C3P006 at the UHF/6-311G*, UHF/6-31G(2d), and MP2/6-311G* levels. Bond distances are in angstrom units.

in the near future, provided enough supercomputer time is available to the authors.

B. Cyclic-linear barrier

When the basis set is enlarged from 6-31G* to 6-311G*, the cyclic isomer (C3P006) is favored, lying 0.81 kcal/mol below the linear structure (C3P003) at the QCISD(T)/6-311G*//HF/6-311G* level (see Table IV). When triple ex-

citations are neglected, the separation increases to 9.80 kcal/mol; this again illustrates the exceptional importance of triple excitations for this potential surface. As expected from the large geometry change, the use of MP2/6-311G* reference geometries increases the separation: it is 1.13 kcal/mol at the QCISD(T) level. The separation is 2.07 kcal/mol at the CCD(ST) level; given the large difference between CCD(S) and QCISD energies, this implies that the errors cancel to a large extent between linear and cyclic states. It

TABLE IV. Total (hartree; minus sign omitted) and dissociation (kcal/mol) energies of C_3 and C_3^+ using large basis sets (MP2/6-311G* reference geometry unless indicated otherwise).

Species	UHF	CCD	CCD(S)	CCD(ST)	QCISD	QCISD(T)
Total energies						
6-311G*						
$C^+(^2P)$	37.29180	37.36110	37.36157	37.36238	37.36188	37.36248
$C(^3P)$	37.68905	37.76512	37.76551	37.76659	37.76562	37.76669
$C_3(^1\Sigma_g^+)$	113.37616	113.73672	113.74364	113.77084	113.74622	113.77400
$C_3^+(^2\Sigma_u^+)$	112.90870	113.29011	113.30348	113.34836	113.30855	113.35266
^a	112.91034	NA	NA	NA	113.30702	113.34960
$C_3^+(^2B_2)$	112.94485	113.31376	113.32084	113.35165	113.32364	113.35446
^b	112.95760	113.29147	113.30240	113.32731	NA	NA
^a	112.95097	NA	NA	NA	113.32264	113.35088
6-311 + G*						
$C^+(^2P)$	37.29248	37.36196	37.36244	37.36325		
$C(^3P)$	37.68957	37.76599	37.76640	37.76753		
$C_3(^1\Sigma_g^+)$	113.37839	113.74010	113.74710	113.77453		
$C_3^+(^2\Sigma_u^+)$	112.91004	113.29180	113.30524	113.35025		
$C_3^+(^2B_2)$	112.94643	113.31561	113.32275	113.35367		
6-311G(2df)						
$C(^3P)$	37.68968	37.77502	37.77545	37.77738		
$C^+(^2P)$	37.29226	37.36522	37.36574	37.36686		
$C_3(^1\Sigma_g^+)$	113.38333	113.78692	113.79331	113.82449		
$C_3^+(^2\Sigma_u^+)$	112.91647	113.33191	113.34466	113.39308		
$C_3^+(^2B_2)$	112.95384	113.35600	113.36315	113.39720		
Dissociation energies						
6-311G*						
$C_3(^1\Sigma_g^+)$	193.91	276.95	280.57	295.61	281.99	297.38
$C_3^+(^2\Sigma_u^+)$	149.85	250.23	257.84	284.14	260.81	286.64
$C_3^+(^2B_2)$	172.54	265.07	268.73	286.21	270.28	287.77
6-311 + G*						
$C_3(^1\Sigma_g^+)$	194.32	277.44	281.05	296.14		
$C_3^+(^2\Sigma_u^+)$	149.61	249.66	257.28	283.59		
$C_3^+(^2B_2)$	172.45	264.60	268.26	285.74		
6-311G(2df)						
$C_3(^1\Sigma_g^+)$	197.22	289.83	293.02	308.96		
$C_3^+(^2\Sigma_u^+)$	153.64	261.46	268.58	295.84		
$C_3^+(^2B_2)$	177.09	276.58	280.19	298.43		
Combined						
Species	UHF	CCD	CCD(S)	CCD(ST)	QCISD(T) ^c	G1
$C_3(^1\Sigma_g^+)$	197.64	290.32	293.51	309.48	311.26	322.11
$C_3^+(^2\Sigma_u^+)$	153.40	260.88	268.02	295.30	297.80	305.04
$C_3^+(^2B_2)$	177.00	276.11	279.72	297.96	299.52	306.76

^a At UHF/6-311G* geometry.

^b C3P004 at the geometry of C3P006.

^c QCISD(T)_x denotes QCISD(T) values estimated assuming additivity of the basis set extension effects and the QCISD(T)-CCD(ST) difference.

would be interesting to compare the results with those of a full CCSDT⁴² calculation, so the effect of the complete \hat{T}_3 ansatz could be assessed.

Note that the CCD(ST) result for C3P004 at the C3P006 geometry differs very significantly from that for C3P006: this is mainly due to the exceptional importance of \hat{T}_1 effects for heavily spin-contaminated species such as C3P004.

Addition of diffuse functions has a relatively small effect on the separation, favoring the cyclic structure by an additional 0.08 kcal/mol. (It is perhaps worth mentioning that the polarity of the Mulliken charge distribution is reversed with respect to that in Fig. 2; this phenomenon was not seen with any of the other basis sets). Finally, expanding the polarization space to (2df) yields a barrier of 2.59 kcal/mol, which is an increase of 0.52 kcal/mol over the 6-311G* basis set. Assuming additivity of the effects of diffuse and additional polarization functions (which is quite reasonable because of their great similarity), we obtain a separation of 2.67 kcal/mol at the CCD(ST) level; correction for the QCISD(T) effects then finally yields a value of 1.73 kcal/mol.

This difference is of the same order of magnitude as our claimed accuracy for the dissociation energy. However, the *ab initio* determination of total atomization energies (TAEs) is a much more demanding problem than the prediction of energy differences between difficult structures of the same molecule, so the uncertainty on the barrier should be much smaller than that on the TAE. We expect that further enhancement of the basis set, as well as reoptimization of the geometry at a higher level, would result in further increases of the barrier, so the present result is best regarded as a lower bound (at least at the levels of electron correlation considered). This also implies that, at least at the levels of electron correlation involved, the qualitative conclusion that the ground state is cyclic is very unlikely to be wrong.

It should be noted that the $S(\text{CCD}) (= E_{\text{CCD}(S)} - E_{\text{CCD}})$ contribution sinks markedly when the polarization space is increased to (2df). It is not entirely unreasonable to expect $S(\text{QCISD}) (= E_{\text{QCISD}} - E_{\text{CCD}})$ to follow the same trend. Also, in the 6-311G* basis, the ratios between $S(\text{QCISD})$ and $S(\text{CCD})$ are comparable for the two structures: 1.379 for the linear, and 1.395 for the cyclic structure. For neutral C_3 (*vide infra*), a value of 1.373 is found. Now assuming that these ratios are approximately transferable across basis sets, we find extrapolated $S(\text{QCISD})$ contributions of 17.69 and 10.05 millihartrees, respectively, for the linear and cyclic structures, compared to the values of 17.90 and 10.00 millihartrees obtained using plain additivity. This would favor the cyclic structure by an additional 0.16 kcal/mol. Analogous considerations for the \hat{T}_3 effect lead to conclusions not significantly different from assuming plain additivity (the cyclic structure is favored by an additional 0.03 kcal/mol), mainly because the differences between $T(\text{CCD})$ and $T(\text{QCISD})$ are relatively small. Our "best theoretical estimate" for the barrier then becomes 1.92 kcal/mol.

It is very likely that the HF/6-31G* frequencies scaled by a recommended factor of 0.89⁴³ are in error by a substan-

tial amount (especially the bending frequency): however, an estimate of the ZPE difference from them should normally be reliable enough to give an indication. It leads to a barrier at 0 K of 1.21 kcal/mol, or 423 cm^{-1} . This means that, just like triplet methylene,⁴⁴ the molecule will be quasilinear, since one or two quanta in the bending vibration will suffice to yield an effective linear structure. Taking the scaled HF/6-31G* bending frequency as an upper bound and assuming a rigid rotor-harmonic oscillator (RRHO) partition function, we obtain a (100)/(000) population ratio of 0.0332 at room temperature and 0.1047 at 450 K. Combining the fact that 97.68% and 89.53%, respectively, of the molecules will still reside in the (000) state, with the expectation that the "linearized" (100) state will have an extremely low bending frequency with large amplitude motions, the experimental R_x distribution is readily explained. At very high temperatures, high populations of (*nkl*) (*n* > 0) states will combine with the relatively low barrier towards degenerate isomerization to create an extremely floppy molecule system.

C. Dissociation energy of neutral C_3

The MP2/6-311G* bond distance of neutral C_3 is found as 1.3030 Å, in very good agreement with the latest experimental r_e value⁴⁵ of 1.2968 Å. Applying the difference as a correction term, we predict r_e geometries of $r = 1.2983$ Å and ($r = 1.3242$ Å, $\theta = 73.06^\circ$) for linear and cyclic C_3^+ , respectively. Because of small spin-contamination effects discussed above, we expect these values to be too low, rather than too high; a conservative error bar would be ± 0.005 Å.

Peculiarly enough, the difference between QCISD and CCD(S) energies is quite significant (Table IV), unlike what is expected for a closed-shell singlet state. The cause for this is readily found in the low-lying π_g orbitals, which are the source of similar albeit smaller effects in the N_2 molecule, as well as in the $a^1\Sigma_g^+$ state of SiC.⁴⁶

Table IV reveals that addition of diffuse functions has a rather small effect of 0.53 kcal/mol on the ΣD_e [at the CCD(ST) level]. As expected, the contribution of additional polarization functions is rather large at 13.35 kcal/mol. An analogous correction for QCISD(T) higher order effects as discussed in the previous section leads to a ΣD_e value of 311.06 kcal/mol. [Assuming simple additivity of the QCISD(T) correction would lead to the value of 311.26 kcal/mol listed in Table IV.]

The G1 correction then yields a ΣD_e of 321.93 kcal/mol, which should be accurate to ± 2 kcal/mol. As the procedure followed here actually involves much less far-reaching assumptions about higher order effects than conventional G1 theory, the error bar is even a bit conservative. Using experimental frequencies from the JANAF tables,⁴⁷ an RRHO estimate for the zero-point energy results in $\Sigma D_0 = 317.08$ kcal/mol. Combined with $\Delta H_{f,0}^0 [C(g)] = 169.98 \pm 0.11$ kcal/mol from the same source, we obtain a $\Delta H_{f,0}^0$ value of 192.86 ± 2 kcal/mol. The JANAF enthalpy functions for C and C_3 finally lead to a $\Delta H_{f,298}^0 - \Delta H_{f,0}^0$ difference of 2.06 kcal/mol, or a $\Delta H_{f,298}^0 = 194.9 \pm 2$ kcal/mol, in excellent agreement with the experimental value of 196 ± 4 kcal/mol, but with a much smaller error margin. A

previous theoretical determination of Raghavachari and Binkley⁵¹ [scaled CCD(ST)/6-31G* ΣD_e combined with HF/6-31G* frequencies scaled by 0.89] yielded a value of 190 ± 4 kcal/mol. Admittedly our theoretical procedure required roughly twenty times as much computer time. However, C_3 should now be added to the list of cluster molecules for which reasonably accurate thermochemical data are available.

D. Ionization potential of C_3

As the geometries of linear C_3 and C_3^+ are hardly different, the energy difference between both can be taken as the first vertical IP, whereas the energy difference between linear C_3 and cyclic C_3^+ would be the first adiabatic IP. In order to assess the accuracy of the theoretical procedure, let us first consider the carbon atom.

At the CCD(ST)/6-311G* and QCISD(T)/6-311G* levels, the IP of $C(^3P)$ is found to be 11.00 eV (Table V), compared to a very precise experimental determination of 11.26 eV.⁴⁷ Addition of diffuse functions has no significant effect, whereas expansion of the polarization space to (2df) leads to a value of 11.17 eV [at the CCD(ST) level]. Δ SCF values fail obviously (10.81 eV); this is even more the case with Koopmans' theorem values [both IP of $C(^3P)$ and EA of $C^+(^2P)$].

Again at the QCISD(T)/6-311G* level, the VIP1 of C_3 is found to be 11.46 eV, in excellent agreement with the MRCI result of Sunil *et al.*,⁹ obtained using a 6-31G basis set supplemented with a diffuse p function and a contraction of two d functions. \hat{T}_1 effects on the VIP1 amount to a rather high 0.24 eV; triple excitations are even more important, contributing 0.45 eV. Use of the CCD(ST) procedure results in an error of only 0.04 eV. Apparently, the MRCI treatment of Sunil *et al.* includes some dominant triple excitation effects through the choice of the reference space.

Addition of diffuse functions increases the VIP1 by no more than 0.04 eV; however, expansion of the polarization space increases VIP1 by no less than 0.24 eV (Table V). Finally, assuming additivity of corrections, one arrives at a best direct VIP1 of 11.76 eV, which is significantly higher than the Sunil *et al.* result. A G1 correction would then finally lead to a "best theoretical VIP1" of 11.92 ± 0.1 eV. This value is in good agreement with the older experimental result of 12.1 ± 0.3 eV,⁴⁸ but a bit above more recent determinations of 9.98–11.61 eV⁴⁹ and 11.1 ± 0.5 eV.⁵⁰ The adiabatic IP would be 0.08 eV lower at 11.84 ± 0.1 eV, which is in marginal agreement with these determinations (and might imply that the linear–cyclic energy difference predicted in this paper is indeed a lower bound). Raghavachari and Binkley⁵¹ found an adiabatic IP of 11.4 eV at the CCD(ST)/6-31G(2d) level: apparently, the basis set has considerable influence on the result.

As expected, Koopmans' theorem and Δ SCF values are hopelessly out of range: the former even wrongly predicted a $^2\Pi_u$ state for the cation. Oddly, the Koopmans' EA of the cation produces very good VIP values of 11.72 eV at the UHF/6-311G* level, and 11.76 eV at the UHF/6-311 + G* and UHF/6-311G(2df) levels (11.80 eV combined). The cause for this is unclear.

IV. CONCLUSIONS

The potential energy surface of the C_3^+ cation has been investigated using coupled cluster techniques and large basis sets. The results are particularly sensitive towards the level of electron correlation. Spin contamination even produces a "false stationary point" at the UHF/6-31G* level. C_3^+ has a cyclic 2B_2 ground state with predicted geometry $r = 1.3242$ Å, $\theta = 73.06^\circ$ (MP2/6-311G*, empirically corrected bond distance). At the highest level of theory considered, the linear structure ($^2\Sigma_u^+$ state) lies about 2 kcal/mol above the

TABLE V. Ionization potentials of C_3 at various theoretical levels.

Species	UHF	CCD	CCD(S)	CCD(ST)	QCISD	QCISD(T)
6-311G*						
C	10.81	10.99	10.99	11.00	10.99	11.00
C_3 (vert)	12.72	12.15	11.98	11.50	11.91	11.46
C_3 (adia)	11.74	11.51	11.50	11.41	11.50	11.42
6-311 + G*						
C	10.80	10.99	10.99	11.00		
C_3 (vert)	12.74	12.20	12.02	11.54		
C_3 (adia)	11.75	11.55	11.55	11.45		
6-311G(2df)						
C	10.81	11.15	11.15	11.17		
C_3 (vert)	12.70	12.38	12.21	11.74		
C_3 (adia)	11.69	11.73	11.70	11.63		
Species	UHF	CCD	Combined CCD(S)	CCD(ST)	QCISD(T)x ^a	G1
C	10.81	11.15	11.15	11.17	11.17	11.18
C_3 (vert)	12.73	12.43	12.25	11.79	11.76	11.92
C_3 (adia)	11.70	11.77	11.75	11.67	11.68	11.84

^aQCISD(T)x denotes QCISD(T) values estimated assuming additivity of the basis set extension effects and the QCISD(T)-CCD(ST) difference.

ground state: this might imply quasilinearity. There is also a low barrier towards degenerate isomerization: at high temperatures, C₃⁺ will be extremely floppy. Harmonic frequencies (UHF/6-31G*) as well as double-harmonic IR and Raman intensities are given for various structures of C₃⁺. Interesting analogies of C₃⁺ with B₃ and B₂N are pointed out. The heat of formation at 298.15 K, vertical and adiabatic ionization potentials of C₃ are predicted as 194.9 ± 2 kcal/mol, 11.92 ± 0.1 eV, and 11.84 ± 0.1 eV, respectively.

ACKNOWLEDGMENTS

The authors are indebted to the Belgian National Fund for Scientific Research (NFWO/FNRS) for a computer time grant on the IBM 3090/400e VF at the K. U. Leuven, and to Professor J.-M. André of the Facultés Universitaires de Namur (FUN) for an allowance of computer time on the IBM-FPS configuration. JM thanks the NFWO/FNRS for a contract as research assistant. Mr. Frans Van de Ven (K. U. Leuven) and Mr. Bruno Durasse (FUN) are credited for technical assistance. This publication forms a part of research results in a project initiated by the Belgian State—Prime Minister's Office—Science Policy Programming.

- ¹W. Weltner, Jr. and R. J. Van Zee, *Chem. Rev.* **89**, 1713 (1989).
²D. Michalska, H. Chojnacki, B. A. Hess, Jr., and L. J. Schaad, *Chem. Phys. Lett.* **141**, 376 (1987).
³J. M. L. Martin, J. P. François, and R. Gijbels, *J. Chem. Phys.* **90**, 3463 (1989).
⁴P. Botschwina and P. Sebald, *Chem. Phys. Lett.* **160**, 485 (1989).
⁵L. Adamowicz and J. Kurtz, *Chem. Phys. Lett.* **162**, 342 (1989).
⁶M. Vald, T. M. Chandrasekhar, J. Szczepanski, R. J. Van Zee, and W. Weltner, Jr., *J. Chem. Phys.* **90**, 595 (1989); P. F. Bernath, K. H. Hinkle, and J. J. Keady, *Science* **244**, 562 (1989); J. R. Heath, A. L. Cooksy, M. M. W. Gruebele, C. A. Schottenmaer, and R. J. Saykally, *Science* **244**, 564 (1989).
⁷L. N. Shen and W. R. M. Graham, *J. Chem. Phys.* **91**, 5115 (1989).
⁸W. L. Brown, R. R. Freeman, K. Raghavachari, and M. Schlüter, *Science* **235**, 860 (1987).
⁹K. K. Sunil, A. Orendt, K. D. Jordan, and D. J. DeFrees, *Chem. Phys.* **89**, 245 (1984).
¹⁰A. Faibis, E. P. Kanter, L. M. Tack, E. Bakke, and B. J. Zabransky, *J. Phys. Chem.* **91**, 6445 (1987).
¹¹Z. Vager, R. Naaman, and E. P. Kanter, *Science* **244**, 426 (1989).
¹²Z. Vager and E. P. Kanter, *J. Phys. Chem.* **93**, 7745 (1989).
¹³L. Gausset, G. Herzberg, A. Lagerqvist, and B. Rosen, *Astrophys. J.* **142**, 45 (1965).
¹⁴M. J. Frisch, M. Head-Gordon, H. B. Schlegel, K. Raghavachari, J. S. Binkley, C. Gonzalez, D. J. DeFrees, D. J. Fox, R. A. Whiteside, R. Seeger, C. F. Melius, J. Baker, R. L. Martin, L. R. Kahn, J. J. P. Stewart, E. M. Fluder, S. Topiol, and J. A. Pople, GAUSSIAN 88 release C, Gaussian, Inc., Pittsburgh, PA, 1989.
¹⁵J. S. Binkley, M. J. Frisch, K. Raghavachari, D. J. DeFrees, H. B. Schlegel, R. A. Whiteside, E. M. Fluder, R. Seeger, D. J. Fox, M. Head-Gordon, and S. Topiol, GAUSSIAN 86 release C, Carnegie—Mellon University, Pittsburgh, PA, 1987.
¹⁶J. A. Pople, R. Krishnan, H. B. Schlegel, and J. S. Binkley, *Int. J. Quantum Chem. Symp.* **13**, 225 (1979).
¹⁷J. A. Pople, M. Head-Gordon, and K. Raghavachari, *J. Chem. Phys.* **87**, 5968 (1987).
¹⁸An excellent review can be found in: R. J. Bartlett, *J. Phys. Chem.* **93**, 1697 (1989).
¹⁹G. D. Purvis and R. J. Bartlett, *J. Chem. Phys.* **76**, 1910 (1982).
²⁰T. J. Lee, A. P. Rendell, and P. R. Taylor, *J. Phys. Chem.* **94**, 5463 (1990).
²¹J. S. Binkley and J. A. Pople, *Int. J. Quantum Chem.* **9**, 229 (1975).
²²J. A. Pople, J. S. Binkley, and R. Seeger, *Int. J. Quantum Chem. Symp.* **10**, 1 (1976).
²³R. Krishnan and J. A. Pople, *Int. J. Quantum Chem.* **14**, 91 (1978).
²⁴H. B. Schlegel, *J. Chem. Phys.* **84**, 4530 (1986).
²⁵R. Krishnan, J. S. Binkley, R. Seeger, and J. A. Pople, *J. Chem. Phys.* **72**, 650 (1980).
²⁶K. Raghavachari, *J. Chem. Phys.* **82**, 4607 (1985).
²⁷K. Raghavachari, G. W. Trucks, J. A. Pople, and M. Head-Gordon, *Chem. Phys. Lett.* **157**, 479 (1989).
²⁸T. Clark, J. Chandrasekar, G. W. Spitznagel, and P. Von Ragué Schleyer, *J. Comp. Chem.* **4**, 294 (1983).
²⁹M. J. Frisch, J. A. Pople, and J. S. Binkley, *J. Chem. Phys.* **80**, 3265 (1984).
³⁰J. A. Pople, M. Head-Gordon, D. J. Fox, K. Raghavachari, and L. A. Curtiss, *J. Chem. Phys.* **90**, 5622 (1989).
³¹J. M. L. Martin, J. P. François, and R. Gijbels, *J. Chem. Phys.* **90**, 6469 (1989).
³²F. Marinelli and A. Pellegatti, *Chem. Phys. Lett.* **158**, 545 (1989).
³³R. A. Whiteside, R. Krishnan, M. J. Frisch, J. A. Pople, and P. Von Ragué Schleyer, *Chem. Phys. Lett.* **80**, 547 (1981).
³⁴R. S. Mulliken, *J. Chem. Phys.* **23**, 1833 (1955).
³⁵J. M. L. Martin, J. P. François, and R. Gijbels, to be published.
³⁶J. Baker, *J. Chem. Phys.* **91**, 1789 (1989); *Chem. Phys. Lett.* **152**, 227 (1988).
³⁷L. Farnell, J. A. Pople, and L. Radom, *J. Phys. Chem.* **87**, 79 (1983).
³⁸J. A. Pople, M. Head-Gordon, and K. Raghavachari, *Int. J. Quantum Chem. Symp.* **22**, 377 (1988).
³⁹J. M. L. Martin, J. P. François, and R. Gijbels, *Chem. Phys. Lett.* **166**, 238 (1989).
⁴⁰D. J. DeFrees, B. A. Levi, S. K. Pollack, W. J. Hehre, J. S. Binkley, and J. A. Pople, *J. Am. Chem. Soc.* **101**, 4086 (1979); D. J. DeFrees, K. Raghavachari, H. B. Schlegel, and J. A. Pople, *J. Am. Chem. Soc.* **104**, 5576 (1982).
⁴¹E. D. Simandiras, J. E. Rice, T. J. Lee, R. D. Amos, and N. C. Handy, *J. Chem. Phys.* **88**, 3187 (1988) and references therein.
⁴²J. Noga and R. J. Bartlett, *J. Chem. Phys.* **86**, 7041 (1987); **89**, 3401 (1988) (E).
⁴³J. A. Pople, H. B. Schlegel, R. Krishnan, D. J. DeFrees, J. S. Binkley, M. J. Frisch, R. A. Whiteside, R. F. Hout, and W. J. Hehre, *Int. J. Quantum Chem. Symp.* **15**, 269 (1981).
⁴⁴P. R. Bunker, in *Comparison of Ab Initio Quantum Chemistry with Experiment for Small Molecules*, edited by R. J. Bartlett (Reidel, Dordrecht, Boston, 1985), p. 141.
⁴⁵K. H. Hinkle, J. J. Keady, and P. F. Bernath, *Science* **241**, 1319 (1988).
⁴⁶J. M. L. Martin, J. P. François, and R. Gijbels, *J. Chem. Phys.* **92**, 6655 (1990).
⁴⁷M. W. Chase, Jr., C. A. Davies, J. R. Downey, Jr., D. J. Frurip, R. A. McDonald, and A. N. Syverud, *JANAF Thermochemical Tables, Third Edition*, *J. Phys. Chem. Ref. Data* **14**, supplement 1 (1985).
⁴⁸F. J. Kohl and C. A. Stearns, *J. Chem. Phys.* **52**, 6310 (1979).
⁴⁹See "note added in proof" in Ref. 9.
⁵⁰S. K. Gupta and K. A. Gingerich, *J. Chem. Phys.* **71**, 3072 (1979).
⁵¹K. Raghavachari and J. S. Binkley, *J. Chem. Phys.* **87**, 2191 (1987).